UNIVERSITY OF BUCHAREST

FACULTY OF CHEMISTRY

PHYSICAL CHEMISTRY DEPARTAMENT

DOCTORAL THESIS

NEW CHEMICALY MODIFIED ELECTRODES WITH IMPROVED ELECTROCATALYTICAL PROPERTIES

-summary-

Scientific coordinator,

CPI. Dr. Totir Nicolae

PhD. Student,

Teodorescu Florina

Bucharest

2012

CONTENTS

Obtaining, characterisation and applications of electrodes with improved electrocatalytical properties were investigated. In this study conducting copolimer films based on azulene and 3-thiophene acetic acid, boron doped diamnond and ceramic materials were used. These materials have been recieved much attention due to their possible technological (sensors, supercapacitors etc.) and biomedical (biosensors, neural prosthetic devices) applications.

II. Original results

II.2.1 Obtaining, characterisation and applications of modified electrodes with copolymer films based on azulene (AZ) and 3-thiophene acetic acid (3TAA).

Conducting copolymer films based on azulene (AZ) and 3-tiophene acetic acid (3TAA) on different substrates (platinum, gold, transparent tin oxide electrode) using three different supporting electrolytes as tetrabutylamonium hexafluorophosphate (**$TBAPF_6$**), tetrabutylamonium tetrafluoroborate (**$TBABF_4$**) and tetrabutylamonium perchlorate (**TBAP**) in acetonitrile were obtained. The electroactive films based on polyazulene (PAZ) and poly(3-thiophene acetic acid) (P3TAA) exhibited a good redox behavior during p-doping process, behavior sustained also by observed changes in the UV-vis spectra due to modification of the films from the neutral into the doped state. The characterizations were accomplished by cyclic voltammetry (**CV**), electrochemical impedance spectroscopy (EIS), UV-Vis absorption spectroscopy (**UV-VIS**), Fourier transform infrared spectroscopy (**FTIR**), Raman spectroscopy, scanning electron microscopy (**SEM**) coupled **EDAX** (energy dispersive X-ray spectroscopy) and atomic force microscopy (**AFM**). By electrochemical copolymerisation, new electroactive materials with relatively high conductivity and good optical and mechanical properties were obtained.

II.2.1.1 Electrochemical synthesis and characterisation of poly(azulene-*co*-3-tiofen acetic acid). Influence of supporting electrolyte

The copolymer films of poly(AZ-co-3TAA) were obtained by sweeping the working electrode potential both in the potential range from –0.6 to 1.2 V (denoted as narrow copolymer film **FCi**) and –0.6 to 1.8 V (called as wide copolymer film **FCe**), at a 0.05 V/s scan rate at room temperature for 5 consecutive potential cycles. The thickness of the coating was established by integration of the charge passed through the cell during electrochemical copolymerization.

It was evidenced the influence of supporting electrolyte toward copolymer films redox behaviour using CV, EIS, SEM coupled with EDAX.

Electrochemical synthesis and characterisation of poly(AZ-co-A3TA) obtained in narrow potential range (–0.6 la 1.2 V)

The highest spin density occurs at 1- and 3- positions in the case of azulene structure and 2- and 5- positions for thiophene structure, respectively. So, these are the positions of the monomers where the random copolymerization most likely occurs (see fig. 1).

Azulene **3-Thiophene acetic acid**

Fig. 1. The molecular structures of the monomers: azulene and 3-thiophene acetic acid

In the process of electrochemical copolimerisation of AZ and 3TAA, firstly azulene radical cations (polarons) and azulenil dications (bipolarons) are formed which then attacks 2- and 5- positions of 3TAA ring structure.

The cyclic voltammograms recorded during electrochemical coolymerization of 5 mM AZ and 5 mM 3TAA onto Pt electrodes in three different supporting electrolytes ($TBAPF_6$, $TBABF_4$, TBAP) when potential range was scanned between -0.6 and 1.2V the were performed (fig.2).

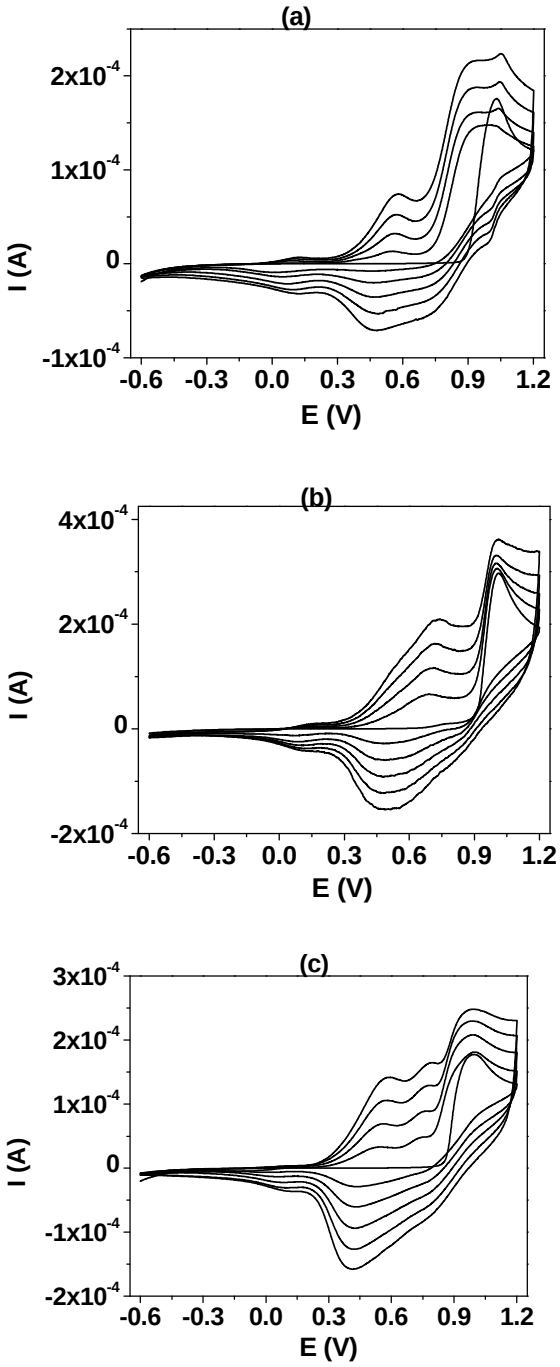

Fig. 2. Copolymerisation of an acetonitrile solution containing 5 mM A3TA, 5mM AZ şi 0.1M a) $TBAPF_6$, (b) $TBABF_4$, (c) TBAP; onto Pt-disc electrode at 50 mV/s when the potential range was scaned between -0.6 and 1.2V.

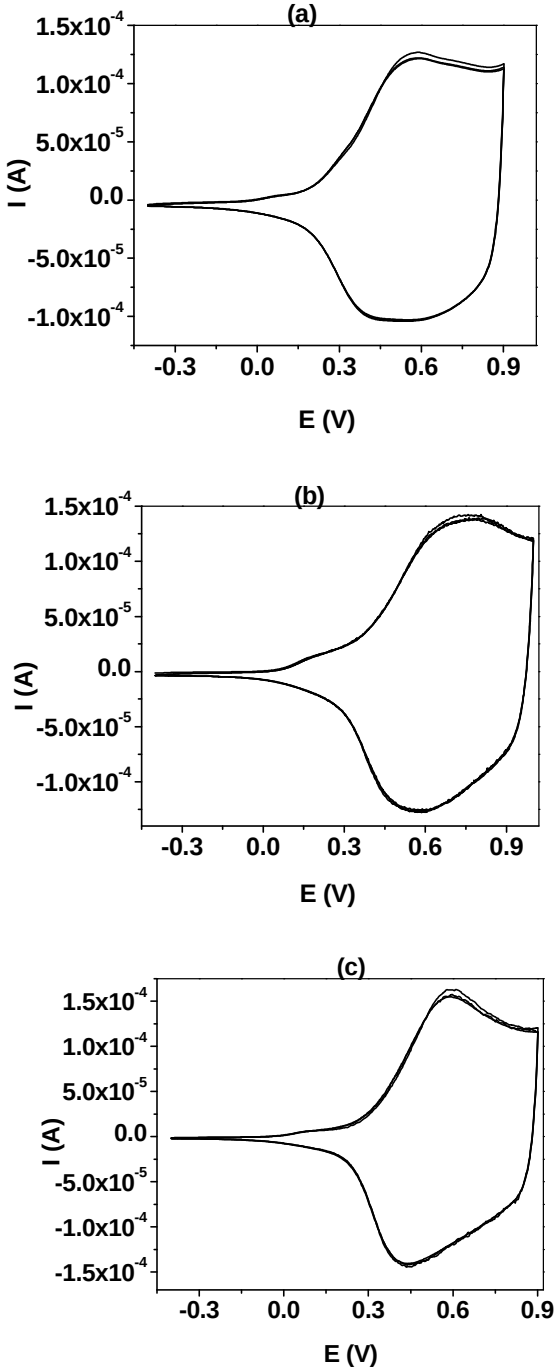

Fig. 3. Cyclic voltammograms recorded for Pt/FCi modified electrodes in transfer solution containing (a) $TBAPF_6$, (b) $TBABF_4$, (c) TBAP în ACN, ν = 50 mV/s

The oxidation peak heights increased with the number of potential scans suggesting that the films were electroactive [1-3].

In fig. 2 a, b şi c, in the first potential scan the oxidation peaks appeared at about 1 V and could be assign to the contribution of both azulene and 3-thiophene acetic acid monomers. Both monomers exhibited close oxidation potentials onto Pt electrodes, E_{AZ}^{ox} =0.96V and E_{3TAA}^{red} =1.08V respectively. In the second potential scan there are two oxidation peaks at 0.54 and 0.96V for $TBAPF_6$, at 0.69 and 1V for $TBABF_4$ and at 0.58 and 0.98V for TBAP, respectively. The first one is associated with the oxidation of the copolymer formed in the first potential cycle and the last is attributed to the contribution of oxidation of the azulene and 3-thiophene acetic acid monomers. During the subsequent potential scans, the peak potentials corresponding both to the copolymer and monomers oxidation does not change significantly The constant increasing of the anodic and cathodic peak currents with successive scans is consisted with the growth of an adherent, conducting and insoluble copolymer film onto Pt electrode.

During the electropolymerization process the counterions of supporting electrolyte and solvent molecules are entrapped into the deposited film on the surface electrode therefore electrochemical properties of the film could be influenced. The synthesized copolymer is formed directly into its conducting state due to the fact that the potential needed for azulene and 3-thiophene acetic acid oxidation is higher than the potentential needed for p-doping process.

The thickness of the copolymer film was controlled by the potential cycle number applied in the electrochemical polymerization process and it was calculated from the integrated charge densities involved in the reaction process, using the following equation:

$$g = \frac{q_{copol} M_{monomeri}}{nFA\rho} \qquad (1)$$

where q_{copol} is the total charge consumed during copolymerization, $M_{monomers}$ is the molar mass of azulene and respectively 3-thiophene acetic acid monomers, *n* represents the number of electrons taking part in oxidation of one monomer unit, *F* the Faraday's constant, ρ is the film density approximated to 1 g/cm^3 and *A* the area of the Au disk electrode surface coated with copolymer film, expressed in square centimeters. For a 3-mm Pt and Au disk electrodes the

surface area was calculated to 0.071 cm^2. The charge density consumed in copolymerization process j_{copol} is expressed in C/cm^2.

The charges consumed in copolymerization reaction, charge density and the thickness of the films obtained in both potential range and in the three supporting electrolytes were computed (table 1).

Table 1. The charges consumed in copolymerization reaction, charge density and the thickness of the copolymer films based on azulene and 3-tiophene acetic acid

Substrate/copolymer film	**Potential range used in copolymerization process***	**Modified electrode abbreviation**	**Supporting electrolyte****	q_{copol} **[10^{-3} C]**	j_{copol} **[C/cm^2]**	**g***** **[µm]**
Pt/poli(AZ-*co*-A3TA)	I (narrow)	Pt/FCi	$TBAPF_6$	7.31	0.10	2.83
Pt/ poli(AZ-*co*-A3TA)	I (narrow)	Pt/FCi	$TBABF_4$	9.46	0.13	3.73
Pt/poli(AZ-*co*-A3TA)	I (narrow)	Pt/FCi	TBAP	6.41	0.09	2.53
Pt/poli(AZ-*co*-A3TA)	II (wide)	Pt/FCe	$TBAPF_6$	18.94	0.27	7.48
Pt/poli(AZ-*co*-A3TA)	II (wide)	Pt/FCe	$TBABF_4$	30.93	0.44	12.21
Pt/poli(AZ-*co*-A3TA)	II (wide)	Pt/FCe	TBAP	17.31	0.24	6.83
Au/poli(AZ-*co*-A3TA)	I (narrow)	Au/FCi	$TBAPF_6$	6.01	0.08	2.37
Au/poli(AZ-*co*-A3TA)	II (wide)	Au/FCe	$TBAPF_6$	14.27	0.20	5.63

* the sweeping of working electrode potential was performed both in the **potential range I** from –0.6 to 1.2 V V vs. Ag/AgCl (denoted as narrow copolymer film **FCi**) and **potential range II,** from –0.6 to 1.8 V (called as wide copolymer film **FCe**)

** it was used the same supporting electrolyte both in electrosynthesis and characterisation processes of copolymer films.

*** in the calculation of copolymer thickness we considered total current efficiency for monomers deposition, not taking into consideration the charge consumed by soluble oligomers.

The electrochemical data obtaind for copolimerisation of AZ and 3TAA onto Au substrate are also included (table 1).

By sweeping the potential in the narrow domain it were obtained thin films. The films thickness varied from 2.53 to 3.73 μm depending on the supporting electrolyte used in the process.

The redox properties of the Au/poly(AZ-co-3TAA) films were studied in the transfer solution containing the same supporting electrolyte as in the copolymerization process. The cyclic voltammograms were recorded during electrochemically oxidation (p-doping) of copolymer films. In CV figures (Fig. 3 a, b, c) the three consecutive scans are shown for the potential window -0.4 V to 0.9V, where the two films are electroactive. The shape of the CVs did not change during scanning of the potential that proves the stability of the films. Both films proved very good electrochemical activity and reversibility during the doping-undoping process. In a p- doping process, the copolymer transition from a neutral to a high conducting state, involve the transfer of both counterions of supporting electrolyte (PF_6^-, BF_4^-, ClO_4^-) and solvent molecules into the film. The electrochemical response for the anodic charging (p-doping) of all three films consisted in symmetric and well defined redox peaks.

The degree of doping y (charge per mole of monomers unit) and the surface concentration of the electroactive sites Γ were calculated according to the following equations:

$$y = \frac{2Q_a}{(q_{copol} - Q_a)}; \qquad (2)$$

$$\Gamma = \frac{Q_a}{yFA_{Au}} \qquad (3)$$

The degree of doping, y is estimated by comparing with the total charge involved in copolymerisation process q_{copol} şi anodic charge Q_a of the copolymer film in the p-doping process.

The degree of doping and the surface concentration of the electroactive sites Γ for the films obtained in both potential range and in the three supporting electrolytes were computed. The values of y and Γ are presented in table 2. The copolymer film obtained in narrow potential range exhibited a higher degree of doping compared with the coatings synthesized in wide potential domain [4]. Studding the influence of supporting electrolyte, **$TBAPF_6$, $TBABF_4$** and **TBAP,** both in the synthesis and in the p-doping processes, the films obtaind in narrow potential domain (FCi) showed better electrochemical properties. The highest value of doping

degree was achieved in the case of the films obtaind in narrow potential domain (FCi) when it was used **$TBAPF_6$** as supporting electrolyte.

Table 2. Anodic charge involved in p-doping processes of the copolymer film Q_a, degree of doping *y* and the surface concentration of the electroactive sites Γ, dependent upon the three suporting electrolytes use in both potential range scans.

Substrate/Copolymer film	**Domeniul de potențial utilizat în procesul de copolimerizare***	**Supporting electrolyte****	Q_a **[10^{-3}C]**	**y**	Γ **[10^{-7} mol/cm^2]**
Pt/FCi	I (îngust)	$TBAPF_6$	1.49	0.51	4.24
Pt/FCi	I (îngust)	$TBABF_4$	0.73	0.17	6.37
Pt/FCi	I (îngust)	TBAP	1.25	0.49	3.76
Pt/FCe	II (extins)	$TBAPF_6$	2.22	0.27	12.20
Pt/FCe	II (extins)	$TBABF_4$	-	-	-
Pt/FCe	II (extins)	TB AP	2.01	0.26	11.16
Au/FCi	I (îngust)	$TBAPF_6$	1.02	0.41	3.64
Au/FCe	II (extins)	$TBAPF_6$	1.66	0.26	9.21

* the sweeping of working electrode potential was performed both in the **potential range I** from –0.6 to 1.2 V V vs. Ag/AgCl (denoted as narrow copolymer film **FCi**) and **potential range II,** from –0.6 to 1.8 V (called as wide copolymer film **FCe**)

** it was used the same supporting electrolyte both in electrosynthesis and characterisation processes of copolymer films.\

Electrochemical synthesis and characterisation of poly(AZ-co-A3TA) obtained in wide potential range (–0.6 la 1.8V)

The films were deposited on Pt electrodes in an acetonitrile solution containing 5 mM AZ, 5 mM A3TA and 0.1 M electrolit suport (**$TBAPF_6$, $TBABF_4$, TBAP**) by sweeping the working electrode potential both in the potential range from –0.6 to 1.8 V, at a 0.05 V/s scan rate at room temperature for 5 consecutive potential cycles. The corresponding voltammograms are illustrated in fig. 4

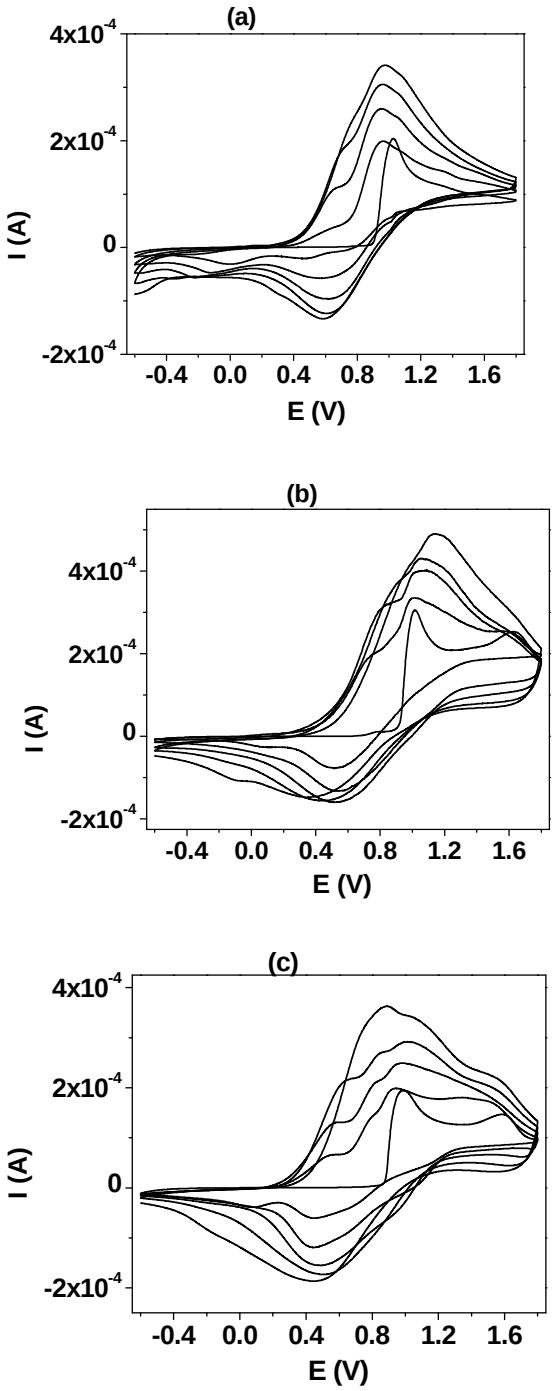

Fig. 4 Copolymerisation of an acetonitrile solution containing 5 mM A3TA, 5mM AZ and 0.1M a) $TBAPF_6$, (b) $TBABF_4$, (c) TBAP; onto Pt-disc electrode at 50 mV/s when the potential range was scaned between -0.6 and 1.8V.

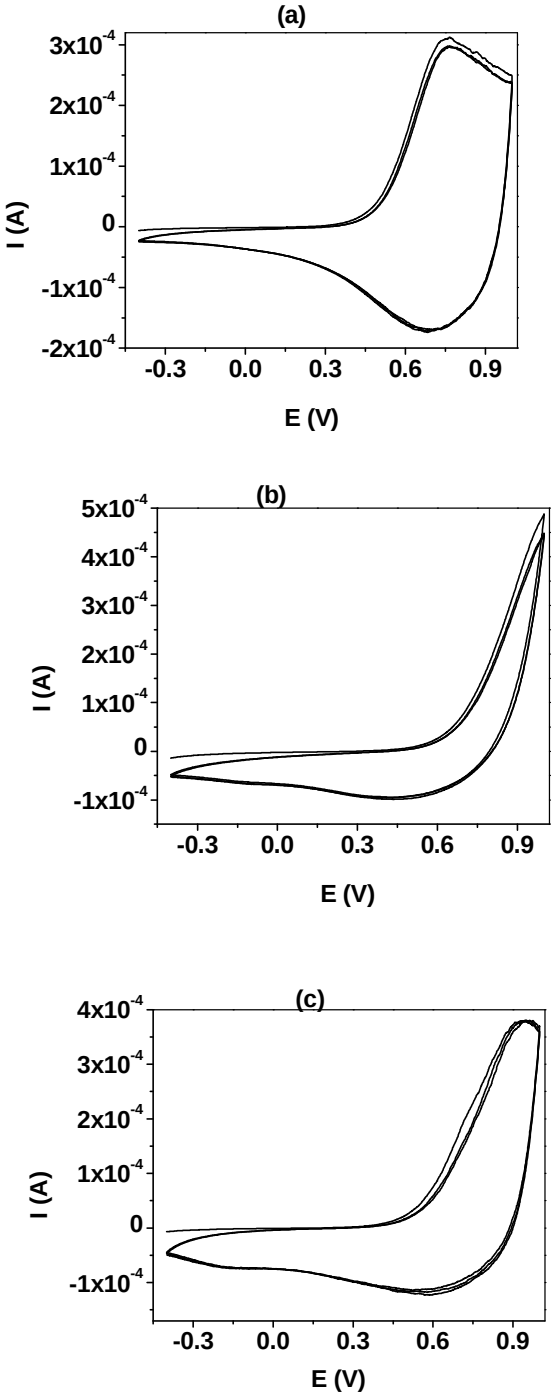

Fig. 5 Cyclic voltammograms recorded for Pt/FCe modified electrodes in transfer solution containing (a) $TBAPF_6$, (b) $TBABF_4$, (c) TBAP în ACN, ν = 50 mV/s

The thicknesses of the films obtained in wide potential range in the three supporting electrolytes were computed (table 1). The thickest copolymer film was obtained for the films obtained in the wide potential domain when it was used $TBABF_4$ as supporting electrolyte. The FCe films exhibited higher charge transfer resistence compared with FCi.

The voltammograms recorded during the FCe characterization in transfer solution containing 0.1M $TBABF_4$ (fig. 5 b) showed that there is no oxidatin peak. This is consisting with the fact that the film demonstrated a high resistance during charge transfer and it exhibited no p-doping behavoiur.

The FCe modified electrode obtained in the presence of $TBAPF_6$ showed the best redox behavoiour during p-doping process; the cyclic voltammograms exhibited a very well-defined anodic and cathodic peaks at 0.76 V and 0.69V vs. Ag/AgCl (fig. 5 a).

The degree of doping and the surface concentration of the electroactive sites Γ for FCe films in the three supporting electrolytes are presented in table 2. The estimated values of y have indicated that the copolymer films obtained by sweeping the potential in wide were less dopable compared with the ones synthesized in narrow potential domain. Studying the influence of supporting electrolyte, **$TBAPF_6$, $TBABF_4$** and **TBAP,** of the films synthesized in wide potential range (FCe) it can be observed that the film obtained in the presence of **$TBAPF_6$** showed the highest values for the doping degree and the surface concentration of the electroactive sites. That's why the following investigations, such as UV-VIS, FTIR, Raman, AFM measurement were accomplished with modified electrodes obtaied in presence of **$TBAPF_6$**.

The electrochemical behavior of the investigated coatings is strongly affected by the thickness and history of the copolymer films. The changes in the morphology of copolymer conducting films containing AZ and 3TAA could be associated with increasing of film thickness and subsequently to different conjugation length. In the case of FCe the effective conjugation length is extended due to the relatively long copolymer chain, the surface is homogenous and the incorporation of anions of the supporting electrolyte into the coating is slower. In the case of WCF the effective conjugation length is a mixture of long and short chain, the surface is homogenous and porous and the incorporation of PF_6^-, BF_4^-, ClO_4^- into the coating is faster.

The cyclic voltmmograms of the modified electrodes with copolymer films for various scan rates were recorded (the figures are illustrated within the thesis). The potential window -0.4 V to 0.9V where the two films are electroactive was employed. During the scan rate changes from 10 to 200 $mV \cdot s^{-1}$ the anodic and cathodic peaks current increased with the increasing of scan rate. This behabiour is indicating a diffusion controlled process for copolymer coatings synthesized in both potential domains.

The diffusion coefficients provided by Randles-Sevcik equation involving the transfer of one electron for both FCi and FCe were determined. These values indicated that PF_6^- diffuses in and out the copolymer film during doping/dedoping processes, faster for the FCe than for the FCi.

The copolymer films for UV-VIS *in situ* spectroelectrochemical measurements were deposited on tin oxide (TO) glass by potential cycling on both potential ranges at 50 mV/s scan rate. In order to avoid the high absorbances in UV-Vis measurements the films were made much thinner than in the CV studies. The copolymer films deposited onto Au electrodes were investigated [4]. The cyclic voltammograms recorded both in the copolymerisation and p-doping processes onto TO and Au substrate are illustrated in thesis.

II.2.1.2 The characterisation by electrochemical impedance spectroscopy (EIS)

The impedance data of the investigated copolymer coatings Fci and FCe were obtained in a monomer free solution at various dc applied potentials ranging between -0.5V and 1.4V(vs. Ag/AgCl), with an increment of 0.1V. The correlations between supporting electrolyte ($TBAPF_6$, $TBABF_4$ şi TBAP) and electroactive properties of conducting copolymer based on AZ and 3TAA were studied.

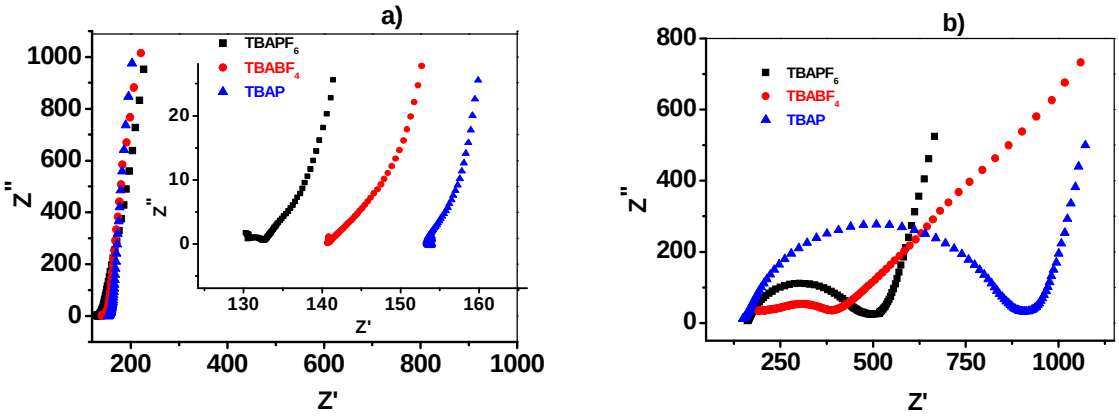

Fig. 6 Nyquist plots for **a)** Pt/FCi and **b)** Pt/FCe**,** in corresponding transfer solutions; E_{apl} = 0.7V; Frequency range: 100 kHz to 100 mHz. Amplitude of alternative voltage was 10 mV.*Inset* Nyquist plots in high frequency range

The films synthesized in the wide potential range exhibited a resistive behaviour, showing a high impedance in medium frequency range The copolymeric films obtained in the narrow potential range in the presence of $TBAPF_6$ as supporting electrolyte exhibited the smallest charge transfer resistance.

In the potential range between -0.5 and 0.3 V vs. Ag/AgCl the copolymer film obtained on both potential domains is an electronic insulator. In this region a purely resistive behaviour of the films is observed and no ionic transfer occurs.

In the potential range between 0.4V and 0.9V vs. Ag/AgCl, both films (FCi and FCe) are in conducting state (fig. 4). In this region the copolymer film undergoes a transition to the best conducting state. The increase in the conductivity of FCi may be attributed to the increase of the effective conjugation length. The extension of effective conjugation length facilitates easy flow of charge between coating and electrode surface. The best conducting potential was found to be 0.7 V for both FCi and FCe, proved by the fact that the coatings exhibit the smallest diameter of semicircle in Nyquist plot, and in consequence the low charge transfer resistance. The R_{ct} values for FCe are higher than the values obtained for FCi. The Rct high value obtained for FCe compared with FCi is due to the increasing of the thickness of the film.

In the potential range between 1V and 1.4V vs. Ag/AgCl, the copolymer films are overoxidized and became electrochemically inactive. In this region a purely resistive behavior of the coatings is displayed and no ionic transfer is evidenced.

The charge transfer conductivity of the copolymer films (σ) was estimated from impedance data. The best conductivity was found to be for FCi ($4.20 \cdot 10^{-3}$ S/cm) [4, 5].

.

II.2.1.3 Caracterizarea prin spectroscopie de absorbție în ultraviolet şi vizibil (UV-VIS)

The UV-VIS absorption spectra of the modified electrodes with poly(AZ-*co*-3TAA) films (TO/FCi and TO/FCe) in a monomer free solution containing 0.1 M $TBAPF_6$/acetonitrile are shown in Fig.7. The *in situ* UV-VIS spectral series were recorded for the copolymer film during the switching process from the reduced state to the oxidized state. The applied potential range was from 100 mV to 1100 mV, with an interval of 100 mV [6].

In the reduced state, the color of the copolymer film was light golden brown and had a single absorption band at 450 nm due to the $\pi - \pi^*$ transition. The increasing of the absorption band at 550 (FCi) and 575 (FCe) nm is associated with the polaron formation. The increasing of the absorbance at 1000 (FCi) and 1040 (FCe) nm for higher oxidation potential is due to the bipolaron formation.

The UV-Visible results demonstrate that FCe exhibited a higher delocalization of π-electrons in the system meaning a higher effective conjugation length (ECL).

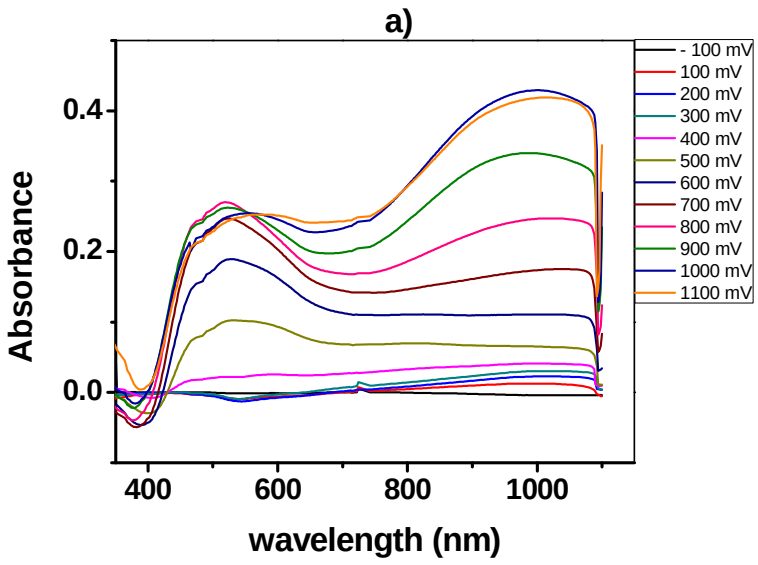

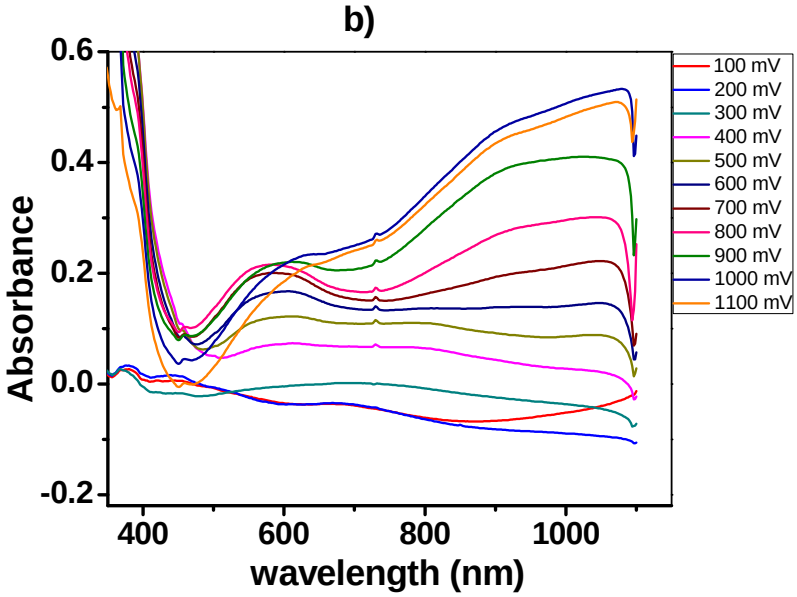

Fig. 7. UV-VIS spectra of a) **TO/FCi**; b) **TO/FCe** in monomer free solution containing 0.1 M $TBAPF_6$ in ACN at various applied potentials

Energy bandgaps (E_g) were estimated based on results from UV-Vis absorbtion spectroscopy and and cyclic voltammetry. The values of the copolymer bandgaps estimated from spectral data were faund to be higher than those calculated from electrode potentials of p- and n-doping processes. The difference is explained based on charge transfer in and out copolimer film during the doping processes.

Diagram of energy levels for copolymer films estimated based on CV measurements recorded during doping processes is depicted in fig. 8.

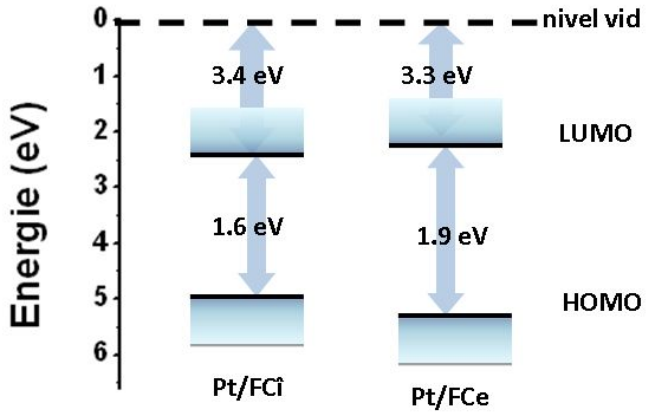

Fig. 8. Diagram of energy levels for copolymer films FCi and Fce, based on CV data recorded during doping process.

II.2.1.4 Characterisation by Fourier transform infrared spectroscopy (FTIR)

FTIR spectroscopy method was used for the characterization of PAZ, AP3TA and poly(AZ-*co*-3TAA) films. The films were deposited onto a Pt substrate in an acetonitrile solution containing the coresponding monomers and $TBAPF_6$ as supporting electrolyte, during 5 consecutive cycles at a scan rate of $0.05Vs^{-1}$. The recorded spectra are illustarated in fig. 9.

.

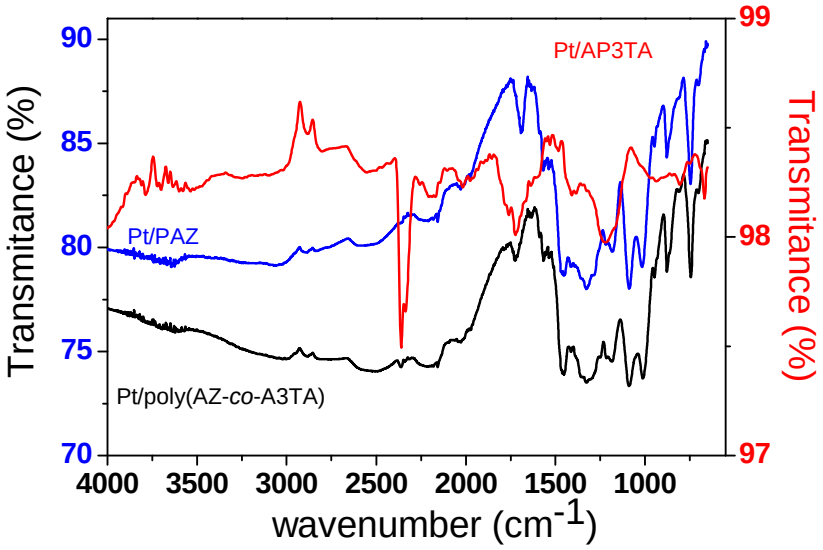

Fig. 9 FTIR spectra of PAZ, AP3TA and poly(AZ-*co*-3TAA) film deposited onto Pt substrate. The films were obtained in CV by sweeping the working electrode potential from –0.6 to 1.8 V

The spectroscopic measurements evidenced the existence of carboxylic group arround 1720 cm^{-1} both in Pt/3TAA and Pt/poly(AZ-*co*-3TAA) films. The presence of COOH group confirm the fact that 3-thiophene acetic acid is incorporated in the structure of copolymeric films.

The copolymer structure contains both azulene and 3-thiophene acetic acid due to the occurrence in FTIR spectra of new vibrations characteristic to azulene and thiophene rings.

II.2.1.5 Characterisation by Raman spectroscopy

Raman spectra of the two films Pt/poly(AZ-co-A3TA), Pt/FCi ($TBAPF_6$) and Pt/FCe ($TBAPF_6$), are illustrated in the Fig.10. Results of the spectra deconvolution procedure are depicted in Table 3.

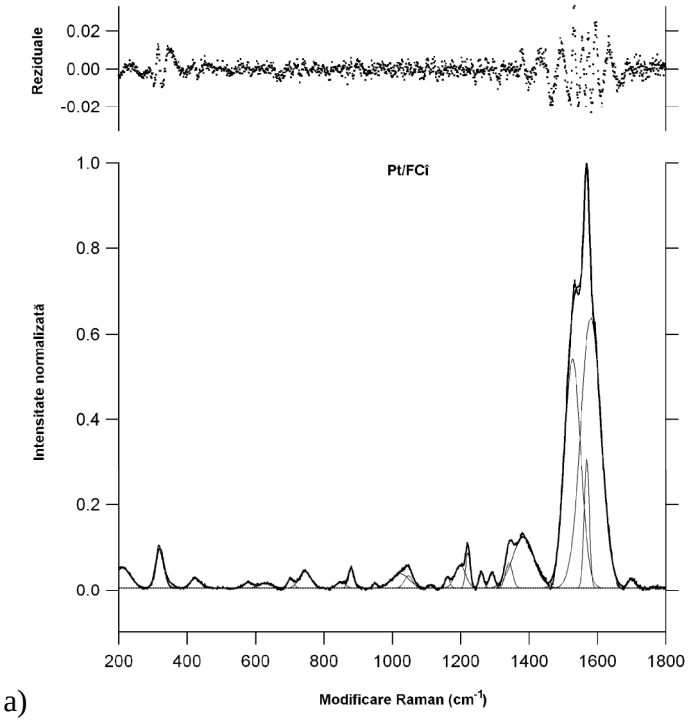

a)

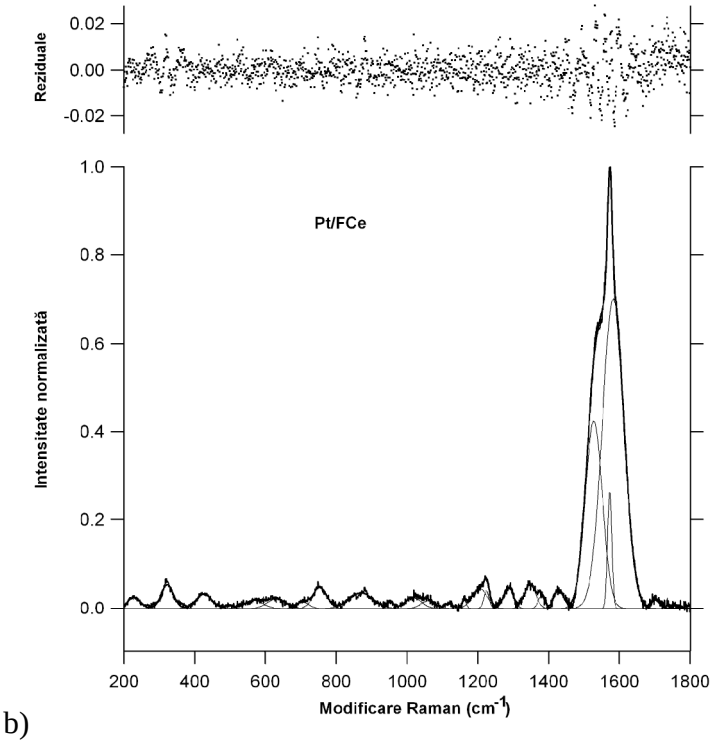

b)

Fig. 10. Deconvoluted Raman spectra of a) **Pt/FCi** and b) **Pt/FCe**

Tabelul 3. Deconvolution results (peak position, FWHM) and literature assignments of the Raman bands for the two (PAZ-co-3TAA)/Pt films

Peak (cm^{-1})	FWHM (cm^{-1})	Peak (cm^{-1})	FWHM (cm^{-1})	Assignment
Film FCi		**Film FCe**		
424	34	426	52	COOH groups
		496	26	in plane ring bending in AZ
579	30	568	59	in plane ring bending in AZ
628	45	631	59	in plane deformation $(C\text{-}C)_{ring}$ in polythiophene
702	20	706	39	C-S-C in plane deformation in polythiophene
745	39	753	45	C-S-C in plane deformation in polythiophene
849	29			C-H out-of-plane deformation in polythiophene
879	19	870	78	OH groups
949	13	952	19	C-H out-of-plane deformation in polythiophene
1022	59	1017	54	symmetric bending of the C-H bonds in β-position of the thiophene rings
1047	29	1059	47	symmetric bending of the C-H bonds in β-position of the thiophene rings (the D band)
1111	15	1118	25	symmetric bending of the C-H bonds in β-position of the thiophene rings (the C band)
1161	17	1162	13	antisymmetric stretching C-C in polythiophene
1198	36	1205	49	Out-of-plane bending C-H
1221	15	1224	18	interring stretching C-C in polythiophene
1260	16			C-C stretching vibrations
1291	20	1287	31	***D*** modes (graphite edges) in AZ
1341	29	1347	37	Stretching $(C\text{-}C)_{ring}$ in polythiophene
1383	54	1379	21	B band of the intra-ring C-C stretching modes in thiophene and bending modes of the hydroxyl group of the carboxylic acid
1426	34	1429	32	Stretching of the C=C bond ring of radical thiophene cations (quinoid)
1527	55	1528	56	symmetric stretching vibration of the aromatic C=C ring bond of polythiophene (band A)
1568	18	1572	14	***G*** modes (graphite lattice) in AZ
1580	69	1582	71	bending modes of the hydroxyl group of the carboxylic acid
1700	23	1701	26	carbonyl group C=O of the 3TAA

The bands at about 1700, 1580, 1383 and 424 cm^{-1} can originate from the carbonyl group C=O of the 3TAA, OH and COOH of the carboxylic acid groups.

Due to the red-shift D modes (at about 1290 cm^{-1}) of the azulene segments in the two films in comparison to the neutral ones (1363 cm^{-1} [3]), the π-electron conjugation between azulene and the thiophene rings could be a plausible explanation.

The Raman spectroscopy measurements evidenced that both azulene and 3-thiophene acetic acid units are included in the structure of the copolymer films.

II.2.1.8 Applications of modified electrodes with copolymer films

II.2.1.8.1 . Electrochemical detection of hydrogen peroxide

The electrocatalytic oxidation of H_2O_2 at Pt/poly(Az-*co*-3TAA) obtained in wide potential range using the three type of supporting electrolytes $TBAPF_6$, $TBABF_4$ and TBAP is studied. The square wave voltammograms of Pt electrode and Pt/poly(Az-*co*-3TAA) electrode, in 0.1 M PB, pH = 6.82, containing different H_2O_2 concentrations: 20, 40, 60, 80, 100, 120, 140 nM were recorded.

In fig. 11 are depicted calibration curves for electrochemical detection of H_2O_2 at Pt/FCe($TBAPF_6$), Pt/FCe($TBABF_4$) and Pt/FCe(TBAP). The modified electrodes synthesized in the presence of $TBAPF_6$, Pt/FCe($TBAPF_6$), exhibited a distinct advantage of specificity and stability.

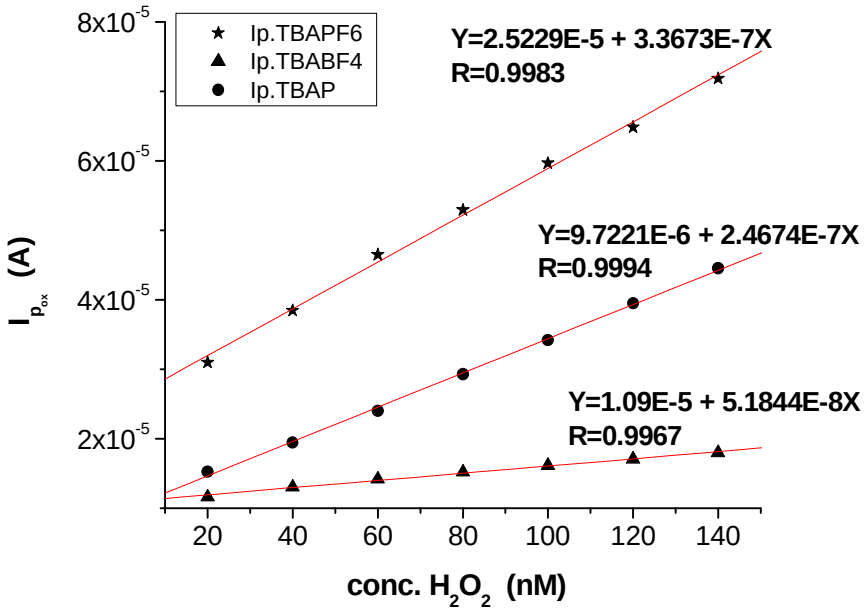

Fig. 11 Calibration curves for Pt/FCe(TBAPF$_6$), Pt/FCe(TBABF$_4$) and Pt/FCe(TBAP) in 0.1 M PB (pH = 6.82), containing different H_2O_2 concentrations: 20, 40, 60, 80, 100, 120, 140 nM

The electrocatalytic oxidation of H_2O_2 at Pt/FCe is studied and compared with unmodified platinum electrode. Fig.12 shows the square wave voltammograms recorded during the oxidation of hydrogen peroxide at Pt electrode and Pt/FCe electrode in 0.1 M phosphate buffer solution with different H_2O_2 concentrations.

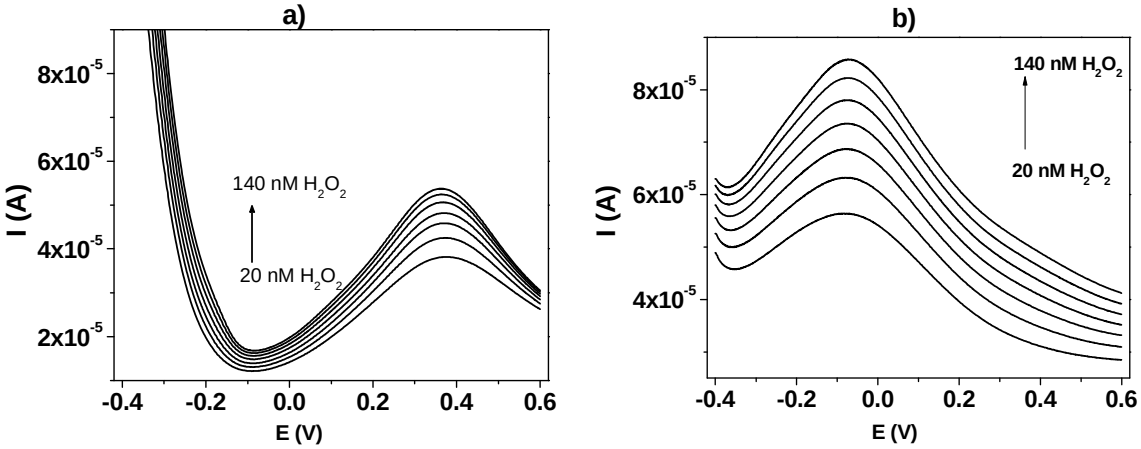

Fig. 12 Square wave voltammograms of **a)** Pt electrode and **b)** Pt/poly(Az-*co*-3TAA) electrode, in 0.1 M PB, pH = 6.82, containing different H_2O_2 concentrations: 20, 40, 60, 80, 100, 120, 140 nM. Pulse amplitude 0.15 V, potential step 0.0015 V, frequency 20 Hz.

The modified Pt/FCe($TBAPF_6$) electrode exhibited higher electrocatalytic oxidation current and lower oxidation potential (-0.07 V) comparing to unmodified platinum electrode (0.36V). By comparison, the Pt/FCe($TBAPF_6$) showed excellent electrocatalytic properties, lower overpotential and higher electrocatalytic current; the possible interference of H_2O_2 with different species is diminished due to the electronegative value of H_2O_2 oxidation potential. The anodic current peak increased with the increasing of H_2O_2 concentration in the range 20 – 140 nM.

II.2.1.8.2 Electrochemical detection of glucose

Glucose oxidase (GOx) was immobilized covalently through carboxyl group of the copolymer films. The amperometric response towards glucose detection of Au/WCF/Gox at various applied potential (0.35, 0.10 and -0.07 V) is studied. Optimal conditions for the enzyme immobilization were investigated and the biosensor was tested for glucose sensing within the concentration range of 10-1000 µM D-glucose. A linear response of the modified enzyme electrode to glucose in the range 40-200 µM was obtained. The best response was achieved when the applied potential was -0.07V vs. Ag/AgCl and a sensitivity of 0.7 nA $cm^{-1}\mu M^{-1}$ was obtained. The detection limit was found to be 27.65 µM [4].

The response of the Au/WCF/Gox biosensor to such cathodic potential is a great achievement due to the fact that the effect of interference such as ascorbic acid, uric acid, dopamine etc is avoided.

II.2.2 Determination of dopamine (DA) and ascorbic acid (AA) using boron doped diamond microelectrode arrays (BDD-MEA)

A selective electrochemical method was developed for the determination of dopamine (DA) and ascorbic acid (AA) using boron doped diamond microelectrode arrays (BDD-MEA). The overlap problem of oxidation peaks for determination of DA and AA in their mixture is solved by using BDD MEA, a good peaks separation of 410 mV between DA and AA was obtained. Thus, the selective determination of DA and AA was carried out with low detection limit, 0.044

μM and 7.5 μM, respectively (S/N=3). The linear range for DA and AA concentration was 0.2 - 1 μM and 20-200 μM, respectively [7].

II.2.3 Ceramic electrodes based on doped lanthanum manganites $La_{0.67}Ca_{0.33}Mn_{1-y}B_yO_3$ (where $y = 0.02$ for B=Fe, Co; y=0,05 for B=Al)

La(Ca)-Mn(Fe, Co, Al)-O type ceramic materials were studied in order to find new routes for modifying and improving its electrocatalytical properties. The key point is the thermodynamic characterization and the correlation of thermodynamic properties with defects chemistry and charge ordering.

The solid state electromotive force measurements (EMF) were employed in order to obtain the thermodynamic properties represented by partial molar free energies ($\Delta\overline{G}_{O_2}$), entalphy ($\Delta\overline{H}_{O_2}$) and entropy ($\Delta\overline{S}_{O_2}$) of oxygen dissolution in the perovskite phase, as well as the equilibrium partial pressures of oxygen (p_{O_2}). The thermodynamic properties evidenced significant changes in the overall concentration of defects depending on the nature of the substituent.

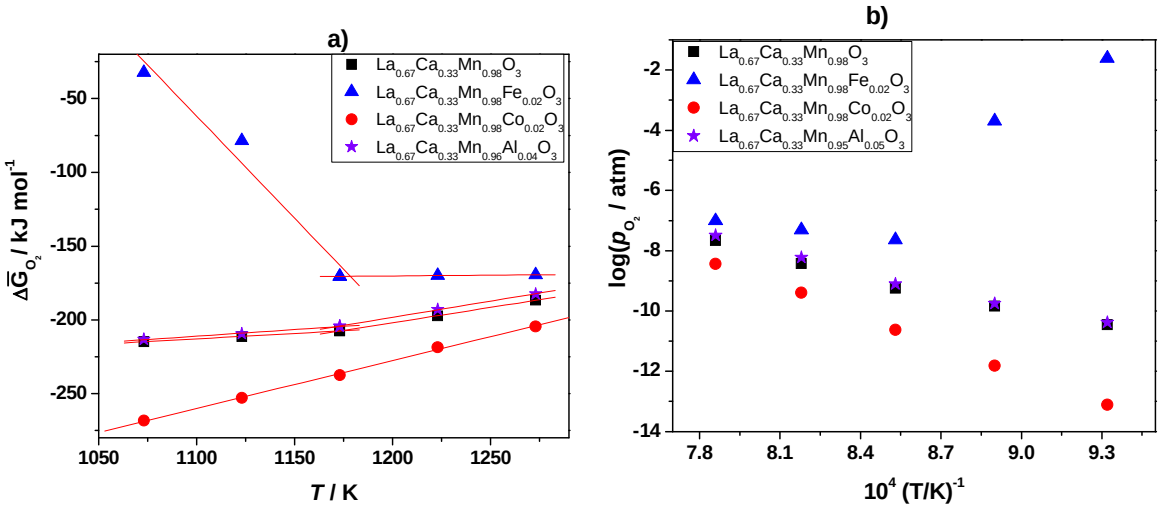

Fig. 15. Variation of $\Delta\overline{G}_{O_2}$ (a) and log p_{O_2} (b) with temperature and samples composition

The variation of $\Delta\overline{G}_{O_2}$ and $log\, p_{O_2}$ of the rare-earth manganites substituted in A-site with Ca and in B-site with Fe, Co and Al in the temperature domain between 1073-1273 K were represented in figure 15.

The highest values of $\Delta\overline{G}_{O_2}$ and p_{O_2} were obtained in the case of samples containing 2% Fe, suggesting that oxygen vacances were easly formed in this compounds. A higher oxygen vacancy means more carriers for oxygen transport, therefore a higher oxygen conductivity is expected. For unsubstituted in B-site $La_{0.67}Ca_{0.33}MnO_3$ sample, as well as for Fe and Al-substituted compounds, two temperature domains were noticed, 1073-1173K and 1173-1273K respectively, where partial molar free energies had liniar variation with temperature. In the 1073-1173 K temperature range, for both $La_{0.67}Ca_{0.33}MnO_3$ and $La_{0.67}Ca_{0.33}Mn_{0.95}Al_{0.05}O_3$, the values of $\Delta\overline{G}_{O_2}$ and $\log p_{O_2}$ are closed each other.

Between 1173-1273K, the values of $\Delta\overline{G}_{O_2}$ and p_{O_2} increase for all the investigated samples, reaching practically similar values around 1273 K. This behaviour could be explained by the fact that in the investigated temperature range the intrinsic deffects are predominant over the impurities defects.

Investigating the effect of B-site substituents (Fe, Co and Al) in $La_{0.67}Ca_{0.33}Mn_{1-y}B_yO_3$ (where $y = 0.02$ for B=Fe, Co; y=0,05 for B=Al), a phase transition at aprox. 1173K for Fe and Al - doped compounds was obtained. This could be associated with orthorombic *(Pbnm)* to hexagonal (*$P6_3cm$)* phase transition.

It was observed that in the investigated temperature range, the 2% Cobalt doped compound is thermodynamically stable, without phase transitions.

Table 4. Relative partial molar thermodynamic data of oxygen dissolution for microstructured compounds substituted in La-site with Ca and in Mn-site with Fe, Co and Al, respectively (temperature range 1073-1273 K)

Compound	**Temperature range**	$\Delta\overline{G}_{O_2} = \Delta\overline{H}_{O_2} - T\Delta\overline{S}_{O_2}$	
		$-\Delta\overline{H}_{O_2}$ **(kJ /mol)**	$\Delta\overline{S}_{O_2}$ **(kJ / mol K)**
$La_{0.67}Ca_{0.33}MnO_3$	1073-1173 K	293.951 ± 3.529	-0.074 ± 0.003

$La_{0.67}Ca_{0.33}MnO_3$	1173-1273 K	451.523 ± 5.468	-0.208 ± 0.004
$La_{0.67}Ca_{0.33}Mn_{0.98}Fe_{0.02}O_3$	1073-1173 K	-1459.824 ± 296.108	1.383 ± 0.263
$La_{0.67}Ca_{0.33}Mn_{0.98}Fe_{0.02}O_3$	1173-1273 K	182.557 ± 1.483	-0.010 ± 0.001
$La_{0.67}Ca_{0.33}Mn_{0.98}Co_{0.02}O_3$	1073-1273 K	616.299 ± 8.927	-0.323 ± 0.007
$La_{0.67}Ca_{0.33}Mn_{0.95}Al_{0.05}O_3$	1073-1173 K	309.082 ± 8.499	-0.089 ±0.007
$La_{0.67}Ca_{0.33}Mn_{0.95}Al_{0.05}O_3$	1173-1273 K	461.784 ± 6.641	-0.219 ± 0.005

The partial molar enthalpies $\Delta\overline{H}_{O_2}$ and entropies $\Delta\overline{S}_{O_2}$ of perovskite solid solution were calculated for temperature ranges where partial molar free energies are linear functions of temperature. The corresponding values $\Delta\overline{H}_{O_2}$ and $\Delta\overline{S}_{O_2}$ are independent of temperature (table 4). In the same temperature range the Gibbs partial molar energy is strongly dependent on the ionic radii of the substituent.

At temperature lower than 1173 K, the Fe doped lanthanum manganites showed the highest values of partial molar enthalpies and entropies; then the values of $\Delta\overline{H}_{O_2}$ and $\Delta\overline{S}_{O_2}$ decrease and are closed for the compounds $La_{0.67}Ca_{0.33}Mn_{0.95}Al_{0.05}O_3$ şi $La_{0.67}Ca_{0.33}MnO_3$; the smallest values of $\Delta\overline{H}_{O_2}$ and $\Delta\overline{S}_{O_2}$, respectively were recorded for Co-doped compound. This suggest that the highest value of binding energy of oxygen was observed for $La_{0.67}Ca_{0.33}Mn_{0.98}Co_{0.02}O_3$, indicating also an increase of order in oxygen sublattice of the perovskite-type structure.

At temperatures higher than 1173 K, it could be observed that the $La_{0.67}Ca_{0.33}Mn_{0.98}Fe_{0.02}O_3$ compound showed the highest $\Delta\overline{H}_{O_2}$ and $\Delta\overline{S}_{O_2}$ variation of all B-site doped manganite samples. The results indicated that oxygen vacancies distribute randomly on the oxygen sublattice in investigated temperature range. It is also interesting to note that the value of $\Delta\overline{H}_{O_2}$ was bigger for the sample $La_{0.67}Ca_{0.33}Mn_{0.98}Fe_{0.02}O_3$ compared with $La_{0.67}Ca_{0.33}MnO_3$, witch is consisting with a small thermic stability of Fe-doped manganite [8-12].

III. Conclusions

- **Development of new chemically modified electrodes based on azulene and 3-tiophene acestic acid. The obtaining coatings were used as senzor/biosensors for hydrogen peroxide and glucose detections.**

The formation and properties of novel redox–active films based on azulene and 3-thiophene acetic acid were investigated. The obtained electroactive coatings exhibited good doping-undoping redox behaviour.

The influence of the yielding potential range and suporting electrolyte, on the redox behaviour of new copolymers films based on AZ and 3TAA was investigated using cyclic voltammetry (CV), electrochemical impedance spectroscopy (EIS), UV-Vis absorption spectroscopy (UV-VIS), Fourier transform infrared spectroscopy (FTIR), Raman spectroscopy, scanning electron microscopy (SEM) and atomic force microscopy (AFM).

The CV, EIS and UV-Vis measurements have been well suited for studying and control the transport of ions during the redox process of the new copolymer films, FCi and FCe. Thus, the CV findings for FCi and Fce in three different supporting electrolytes ($TBAPF_6$, $TBABF_4$, TBAP) show that the doping/dedoping process consists in a reversible exchange of anions. Also, EIS and UV-Vis data for FCi and FCe in $TBAPF_6$ indicated a higher effective conjugation length for the former film.

Electrocatalytic properties of Pt/poly(AZ-co-3TAA) toward H_2O_2 detection were conducted. The obtained electrochemical sensor showed a linear response to hydrogen peroxide over concentrations range from 20 to 140 nM with a sensitivity of 0.2 μA/nM. The limit of detection based on three times the noise level (S/N=3), was determined to be 10.5 nM.

Electrocatalytic properties of Au/poly(Az-co-3TAA)/Gox toward glucose detection were demonstrated. The obtained electrochemical sensors showed a linear response to glucose over concentrations range from 40 to 200 μM with a sensitivity of 0.7 nA $cm^{-1}\mu M^{-1}$ at the –0.07 V vs. Ag/AgCl applied potential. The detection limit was 27.65 μM.

- **Development of a selective electrochemical method for the determination of dopamine (DA) and ascorbic acid (AA) using boron doped diamond microelectrode arrays (BDD-MEA).**

The BDD MEA exhibits a good electrocatalytic activity for the oxidation of DA and AA. In voltammetric measurements of DA and AA in their mixture solutions, the separation of the oxidation peak potentials is about 410 mV. BDD MEA presented a linear response range between 0.2 and 1 µM and 20 and 200 µM for determining DA and AA, respectively. This work demonstrates the advantage in utilizing of BDD MEA for selective and sensitive determination of DA over the conventional microelectrodes. Thus, BDD MEA proved to be useful for the content uniformity test of dopamine hydrochloride ampoules, the obtained results indicate that the BDD MEA can be reliable used for the DA determination in pharmaceutical products. The present study requires further research concerning to detection of DA and AA in biological samples.

- **Effect of the nature and concentration of substituents on the thermodynamic properties of microstructured substituted lanthanum manganites** $La_{0.67}Ca_{0.33}Mn_{1-y}B_yO_3$ **(**where $y = 0.02$ for B=Fe, Co; y=0,05 for B=Al**).**

La(Ca)-Mn(Fe, Co, Al)-O type ceramic materials were investigated in order to fiind new routes to modify and to improve its electrocatalytical properties.

Experimental thermodynamical results confirm the solid solution formation due to substitution with Fe, Co and Al.

Partial molar free energies ($\Delta\overline{G}_{O_2}$), as well as the equilibrium partial pressures of oxygen (p_{O_2}) exhibits linear dependence on temperature in defined temperature ranges. In these domains of temperature, the partial molar entalphy ($\Delta\overline{H}_{O_2}$) and entropy ($\Delta\overline{S}_{O_2}$) of oxygen dissolution in the perovskite phase proved to be independent of temperature.

Phase transition at about 1173 K could be associated with orthorombic *(Pbnm)* to hexagonal (*$P6_3cm$)* phase transition for the investigated samples, except for the Co doped one.

The 2% cobalt doped compound is thermodynamically stable in the whole investigated temperature range (1073-1273 K).

This research allowed to obtain new and systematic thermodynamic data for the studied compounds and to highlight the influence of different parameters (like temperature and composition) on the thermodynamic properties.

Understanding the role of charge ordering and the defects chemistry in explaining the thermodynamic behaviour of the investigated manganites, it should be possible to find new routes for modifying the properties of these materials. The doping with different foreign cations proved to be an efficient method to obtain new materials with improved properties (electrical and thermodynamic).

Selected references

[1] F. Teodorescu, C. Lete, M. Marin, N. Totir, International Conference of Physical Chemistry (**ROMPHYSCHEM-14)**, Bucuresti, Romania, 2-4 iunie **2010.**

[2] F. Teodorescu, C. Lete, M. Marin, N. Totir, 6th Chemical Engineering Conference for Collaborative Research in Eastern Mediterranean Countries (**EMCC 6**), Belek -Antalya, Turcia, **2010**

[3] F. Teodorescu, C. Lete, M. Marin, N. Totir, Second Regional Symposium on Electrochemistry, South-East Europe (**RSE-SEE2**), Belgrad, Serbia, 6-10 iunie **2010**.

[4] F. Teodorescu, C. Lete, M. Marin, C. Munteanu, N. Totir, *Rev. Chim.*, 64(1), 15-20, **2013**.

[5] C. Lete, F. Teodorescu, N. Totir, M. Badea-Doni, Third Regional Symposium on Electrochemistry: South ‑ East Europe (**RSE-SEE3**), Bucuresti, 13-17 mai **2012.**

[6] F. Teodorescu, C. Lete, N. Totir, 17th Romanian International Conference on Chemistry and Chemical Engineering (RICCCE 17), Sinaia, Romania, 7-10 septembrie **2011**.

[7] C. Lete, F. Teodorescu, M. Marin, *Rev. Chim.*, acceptat spre publicare, 2013.

[8] S. Tanasescu, F. Maxim, F. Teodorescu, L. Giurgiu, ***J. Nanosci. Nanotech.***, 8(2), 914 – 923, 2008.

[9] S. Tanasescu, M.N. Grecu, M. Urse, F. Teodorescu, L.M. Giurgiu, H. Chiriac, N.D. Totir, ***Adv. Appl. Ceram.***, 108(5), 273 – 279, 2009.

[10] F. Teodorescu, A. Botea-Petcu, S. Tanasescu, 17th Romanian International Conference on Chemistry and Chemical Engineering (**RICCCE 17**), Sinaia, Romania, 7-10 septembrie **2011**.

[11] F. Teodorescu, A. Botea-Petcu, S. Tanasescu, Z. Yáng, J. Martynczuk, L. Gauckler, Third Regional Symposium on Electrochemistry: South ‑ East Europe (**RSE-SEE3**), Bucuresti, 13-17 mai **2012.**

[12] F. Teodorescu, A. Botea-Petcu, Z. Yáng, J. Martynczuk, L. Gauckler, S. Tanasescu, **EUROMAT JUNIOR 2012,** Lausanne (Elveția), 22-28 iulie **2012.**